

1 Subsea natural gas dehydration with membrane processes:  
2 Simulation and process optimization

3 Kristin Dalane, Magne Hillestad\*, Liyuan Deng\*

4 *Department of Chemical Engineering, Norwegian University of Science and Technology (NTNU),*  
5 *Sem Sælandsvei 4, N-7491 Trondheim, Norway*

---

6 **Abstract**

Subsea processing enables broader exploration of oil and gas reservoir, giving an increased focus on developing alternative processes for subsea oil and gas treatment. This work provides a first evaluation of a new proposed subsea natural gas dehydration process with the use of a membrane contactor with triethylene glycol (TEG) for dehydration of the natural gas in combination with thermopervaporation for regeneration of the TEG. Simulation models are developed in Aspen HYSYS V8.6 and process optimization is performed on three different process designs with respect to staging of the regeneration. By introducing two thermopervaporation units in series the TEG flow rate is reduced by 55%, the membrane volume by 14.6% and the energy demands by 37.8%, compared to a design with one thermopervaporation unit. However, increasing the number of regeneration stages increases the complexity as additional heaters are introduced.

7 *Keywords:* Subsea natural gas dehydration, Membrane Contactor, Thermopervaporation, Process  
8 Optimization, Triethylene glycol

---

---

\*Corresponding author.

*Email addresses:* `magne.hillestad@ntnu.no` (Magne Hillestad), `liyuan.deng@ntnu.no` (Liyuan Deng )

9 **Contents**

10	<b>1 Introduction</b>	<b>3</b>
11	<b>2 The proposed process concept</b>	<b>5</b>
12	2.1 Simulation assumptions . . . . .	6
13	2.2 MATLAB CAPE-OPEN unit operation in Aspen HYSYS . . . . .	7
14	2.3 Membrane contactor . . . . .	7
15	2.4 Thermopervaporation unit . . . . .	8
16	<b>3 System optimization</b>	<b>8</b>
17	3.1 Objective function . . . . .	10
18	<b>4 Results and discussion</b>	<b>12</b>
19	4.1 Price sensitivity study . . . . .	16
20	<b>5 Conclusion</b>	<b>18</b>

## 1. Introduction

Natural gas from the reservoir is normally saturated with water, which may condense during transportation causing flow assurance problems such as hydrate formation, corrosion and erosion [1]. Removal of the water can prevent these challenges and dehydration of natural gas is therefore one of the main processing steps in natural gas treatment. Several methods can be used for dehydration of natural gas, such as absorption into a solvent or adsorption onto a solid [2]. The most common technology used in the oil and gas industry today is the absorption process with the use of glycols, typically triethylene glycol (TEG), as illustrated in Fig. 1. The inlet scrubber is applied to remove hydrocarbon liquids and/or free water from the wet gas before it enters the glycol contactor. In the glycol contactor the natural gas meets the glycol in a counter-current flow and the dry gas leaves from the top of the column. The rich TEG (TEG with the absorbed water) is regenerated before it is reused as lean TEG in the glycol contactor. In addition to the topside dehydration facility, injection of hydrate inhibitor such as monoethylene glycol (MEG) or methanol is commonly used to prevent hydrate formation from the reservoir to the topside treatment facility [3].

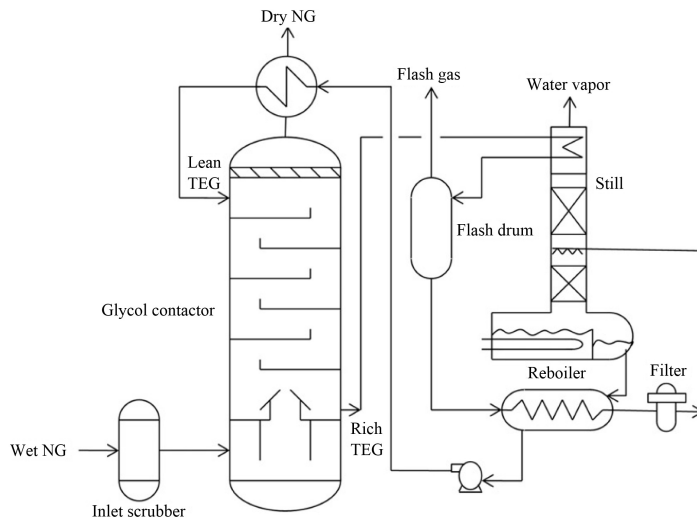


Figure 1: Process design for commonly used natural gas dehydration process with glycol [4]

With increasing focus on subsea processing and the ultimate vision of directly exporting of the produced hydrocarbons from the reservoir to the market [5], alternative technologies for subsea dehydration of natural gas should be investigated. Subsea dehydration can reduce the water content in downstream processing steps to acceptable levels, and eliminate the need for continuously injection of hydrate inhibitor. In addition, subsea dehydration can provide subsea to shore production, as the gas will be processed subsea and directly exported [6]. When considering a technology for subsea installation several design criteria should

40 be considered. Unmanned operation is required as the process is placed at a remote location and limiting  
41 moving parts is favorable to reduce the need for maintenance [7]. With respect to high accessibility and  
42 retrievability, high modularity is preferred. Depending on the water depth of the installation, compact de-  
43 sign is favorable due to the limitations in size and weight for the installation cranes [8, 9]. The complexity  
44 of the system should be kept low and the number of process equipment to a minimum. To avoid leakage  
45 and minimize the potential of failure, the number of subsea connection points should be low, which makes  
46 it important to consider how the process design should be installed in subsea modules.

47  
48 Membrane technology being compact with no moving parts, in addition to flexible operation due to high  
49 modularity make membranes and membrane contactors to interesting technologies for subsea operation [10].  
50 Membrane contactor is a hybrid technology combining the advantages of both absorption and membrane  
51 technology. One of the advantages compared to conventional adsorption columns is the higher surface area  
52 per unit contactor volume, providing increased contact area in a smaller module. During the last decade,  
53 membrane contactors have been intensively studied, especially for CO<sub>2</sub> capture [11–33]. Promising result  
54 have been reported from one pilot test of natural gas dehydration with membrane contactor, showing dehy-  
55 dration to pipeline specification and stable operation [34–36].

56  
57 Regeneration of TEG is commonly achieved with distillation technology, but the system complexity and en-  
58 ergy demand make the process less feasible for subsea operation. This encourage the research for alternative  
59 technologies for subsea regeneration of TEG. Wijmans et al. [37] patented a natural gas dehydration process  
60 where the regeneration step is replaced with vacuum pervaporation. Pervaporation combines permeation  
61 through a membrane with evaporation, leading to a possibly higher recovery of the TEG. In vacuum per-  
62 vaporation, a vacuum pump is applied on the permeate side to achieve a low vapor pressure and improve  
63 the separation performance. An alternative to the vacuum pervaporation; i.e. driving force by vacuum  
64 pump, is thermopervaporation where the low vapor pressure is maintained by condensing the permeate; i.e.  
65 driving force created by temperature differences. The access to large amount of cooling water on the seabed,  
66 makes thermopervaporation an interesting technology for subsea operation. Several researchers [38–56] have  
67 investigated dehydration of monoethylene glycol (MEG) with vacuum pervaporation. Little information is  
68 found on research for dehydration of TEG with vacuum pervaporation [57–59], and no data for thermop-  
69 ervaporation. Due to the limited investigation of membrane contactor for dehydration of natural gas and  
70 TEG regeneration with thermopervaporation, more research is needed to evaluate the potential for subsea

71 operation.

72

73 In this work, a natural gas dehydration process with the use of membrane technology is evaluated through  
74 modelling and simulation. Compared to the commonly used absorption process in Fig. 1, the conventional  
75 packed absorption column is replaced with a hollow fiber membrane contactor unit. In addition, the regen-  
76 eration part is replaced with a thermopervaporation unit. The models of the membrane contactor [60] and  
77 thermopervaporation unit [59] are already published and will not be described here. They are written in  
78 MATLAB and implemented in Aspen HYSYS V8.6 with the use of MATLAB CAPE-OPEN (version 1) [61].  
79 Here, process design with different number of regeneration stages are evaluated, in addition to optimization  
80 of the operation conditions for the system with respect to TEG flow rate and membrane module sizes.  
81 Moreover, the different designs are compared based on subsea feasibility with respect to sizes, number of  
82 stages and energy demands. This is the first and an important step in the feasibility evaluation of the new  
83 proposed dehydration process.

## 84 2. The proposed process concept

85 The proposed subsea natural gas dehydration process is illustrated in Fig. 2 and the selected capacity is  
86 a natural gas feed of 25 MSm<sup>2</sup>/d, saturated with H<sub>2</sub>O at reservoir conditions. Åsgard transport condition  
87 is selected as the dehydration requirements, with a water dew point of -18°C at 69 barg [5, 62]. The  
88 pressure and the temperature of the natural gas from the reservoir are reduced to 80 bar and 25°C and a  
89 scrubber is applied to remove the liquid hydrocarbon and/or free water. The natural gas from the scrubber  
90 is saturated with water, which may condense if the temperature in the pipeline is reduced. Therefore, to  
91 prevent condensing of the water before the membrane contactor inlet, the natural gas is heated to 30°C. The  
92 properties of the wet natural gas feed to the membrane contactor are as given in Table 1. The wet natural  
93 gas enters the membrane contactor on the shell side and the triethylene glycol (TEG) flows counter-current  
94 inside the fibers. The H<sub>2</sub>O is transported over the membrane and absorbed into the TEG, providing a dry  
95 natural gas ready to be exported. The rich TEG is reduced in pressure to 1 bar and heated before it enters  
96 the thermopervaporation unit for regeneration by removal of the water. The regenerated TEG is reused in  
97 the membrane contactor for absorption of H<sub>2</sub>O. Prior to the membrane contactor inlet the temperature and  
98 pressure of the TEG is adjusted to the same conditions as the membrane contactor gas inlet.

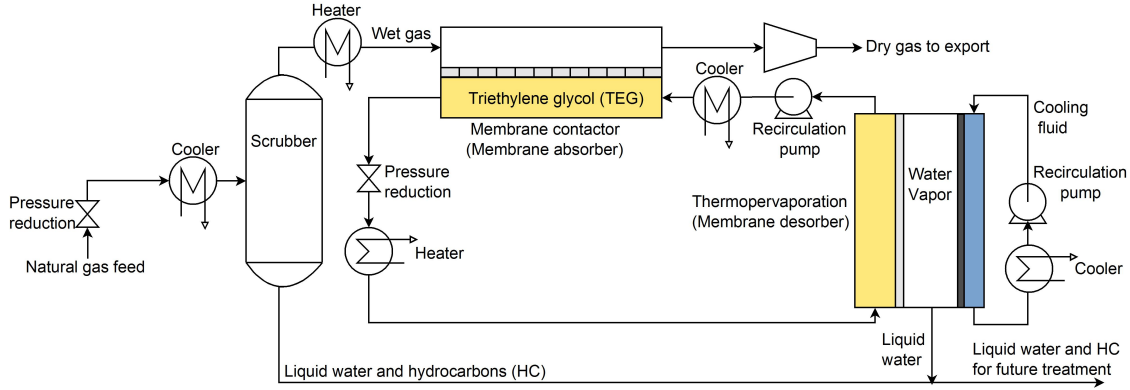


Figure 2: Simplified illustration of the proposed subsea natural gas dehydration system

Table 1: Properties of the wet natural gas for the membrane contactor inlet

Parameter	Value
Temperature [°C]	30
Pressure [bar]	80
Flow [Sm <sup>2</sup> /d]	24.9
Molar flow [kmol/h]	4.4·10 <sup>4</sup>
H <sub>2</sub> O content [ppm]	600

99 *2.1. Simulation assumptions*

100 Simulations are carried out using Aspen HYSYS V8.6 process simulator. Modelling of the membrane contac-  
 101 tor and thermopervaporation unit are performed in MATLAB and implemented into Aspen HYSYS with the  
 102 use of MATLAB CAPE-OPEN (version 1). The other units in the design (scrubber, heaters, coolers, pumps  
 103 and pressure relief valves) are standard units in Aspen HYSYS. The design pressure drop in the scrubber,  
 104 heaters and coolers are assumed to be negligible. The thermodynamic models used to calculated the ther-  
 105 modynamic properties in the simulations are Peng-Robins (PR) for the natural gas and the non-random  
 106 two-liquid model (NRTL) for the liquid phase. With the use of MATLAB CAPE-OPEN it is possible to  
 107 choose if the physical properties of the gas and liquid should be retrieved from Aspen HYSYS properties  
 108 or from defined correlations inside the model. In the developed models, all the physical properties required  
 109 for the TEG and the natural gas are calculated based on defined correlation inside the model. The HYSYS  
 110 flow sheet gives the feed conditions to the membrane modules such as the temperature, the pressure, the  
 111 composition and the total flow rate, and the outlet conditions are provided by the model. Only water is  
 112 assumed to be transported over the membrane in the membrane units.

113

114 *2.2. MATLAB CAPE-OPEN unit operation in Aspen HYSYS*

115 CAPE-OPEN is a standard for communication between chemical engineering software components, faci-  
116 tating interoperability between process simulators. Most simulation software are CAPE-OPEN compliant,  
117 including Aspen HYSYS, which means that a CAPE-OPEN unit operation and property package can be  
118 included in the simulation [63]. CO-LaN is a non-profit organization responsible for the management of the  
119 CAPE-OPEN standard [64]. "MATLAB CAPE-OPEN unit operation" developed by AmsterChem [61] is a  
120 software for developing unit operation models to be implemented in CAPE-OPEN compliant software. This  
121 give the advantage that all the function in the MATLAB library can be used within the simulation software.  
122 In addition to simple implementation of MATLAB models as unit operations.

123 *2.3. Membrane contactor*

124 The membrane contactor model is based on a hollow fiber module configuration with counter-current flow.  
125 On the shell side a one-dimensional model is used for the gas flow. For the liquid in the lumen side, a  
126 two-dimensional model is developed to describe the temperature and the concentration profiles in axial and  
127 radial directions. The partial differential equations describing mass, temperature and pressure changes are  
128 discretized by orthogonal collocation. Consequently this results in nonlinear algebraic equations solved in  
129 MATLAB by Newton-Raphson type iteration. In a previous work, the model was validated against high  
130 pressure experimental data and a sensitivity study with respect to membrane and module properties was  
131 performed [60]. The result from this evaluation provides the selection of membrane and module properties  
132 used for the membrane contactor in this simulation, as listed in Table 2. To meet the subsea requirements  
133 of long-term stable operation, a thin composite membrane has been selected to avoid pore wetting, which  
134 significantly reduces the separation performance. The selected membrane for this process evaluation consist  
135 of a porous polypropylene (PP) support coated with a dense layer of Teflon®AF2400.

Table 2: Specifications of membrane contactor

Parameter	Value	Unit
Fiber inner diameter	600	$\mu\text{m}$
Membrane length	1	m
Packing density	1500	$\text{m}_m^2/\text{m}_t^2$
Membrane thickness (porous, PP)	200	$\mu\text{m}$
Membrane porosity	0.71	
Membrane thickness (dense, AF2400)	1	$\mu\text{m}$
Membrane permeability (dense, AF2400)	3000	Barrer
Operation pressure	80	bar
Operation temperature	30	$^\circ\text{C}$

136 *2.4. Thermopervaporation unit*

137 The thermopervaporation model is based on the plate-and-frame module configuration, with alternated  
 138 channels for the TEG, air gap and the cooling water. The TEG and the cooling water are modelled as  
 139 two-dimensional laminar flow, while the air gap is considered as a stagnant phase. The model consist of  
 140 a temperature dependent permeability correlation for the dense Teflon®AF2400 layer, developed based on  
 141 results from vacuum pervaporation experiments [59]. The same solving methods is used for the thermoper-  
 142 vaporation model as for the membrane contactor. In a previous work a sensitivity study was performed for  
 143 the thermopervaporation unit with respect to membrane and module properties [59]. The selected specifi-  
 144 cations used for this evaluation are based on the results from the sensitivity study, as given in Table 3.

145

Table 3: Specifications of thermopervaporation

Parameter	Value	Unit
Feed channel thickness	4	mm
Air gap	1	cm
Membrane length	1	m
Membrane width	1	m
Membrane thickness (porous, PP)	25	$\mu\text{m}$
Membrane porosity	0.41	
Membrane thickness (dense, AF2400)	1	$\mu\text{m}$
Cooling water channel thickness	5	mm
Cooling water operation temperature	4	$^{\circ}\text{C}$
Cooling water velocity	0.05	m/s
Operation pressure	1	bar

146 **3. System optimization**

147 There are several design variables that can be adjusted to obtain the optimum process design. The goal for  
 148 the process is to meet the dehydration specifications for the dry natural gas, which is a water dew point of  
 149  $-18^{\circ}\text{C}$  at 69 barg. In all the cases the dehydration criteria must be fulfilled. As mentioned above, based  
 150 on the sensitivity analysis of the membrane units the membrane and module parameters are given specific  
 151 values. In addition, a given natural gas feed is used with the conditions as given in Table 1. This leaves  
 152 us with five variable for the optimization of the process design, including TEG flow rate, TEG regeneration  
 153 temperature, membrane contactor size (number of fibers), size of the thermopervaporation unit(s) (number  
 154 of feed channels) and the number of regeneration stages in series.

155



156 The liquid temperature in the thermopervaporation unit will decrease along the module due to heat of  
 157 evaporation and heat transfer between hot and cold fluid. A reduction in the liquid temperature results  
 158 in reduced separation performance. It is possible to improve the separation performance by using several  
 159 stages of the regeneration in series with heating between the stages. Three different process designs with  
 160 respect to number of stages for the regeneration were investigated, including one (Design 1), two (Design 2)  
 161 and three (Design 3) stages. A simplified illustration of the three process designs are given in Fig. 3. The  
 162 remaining variables are then used in the optimization of each process design.

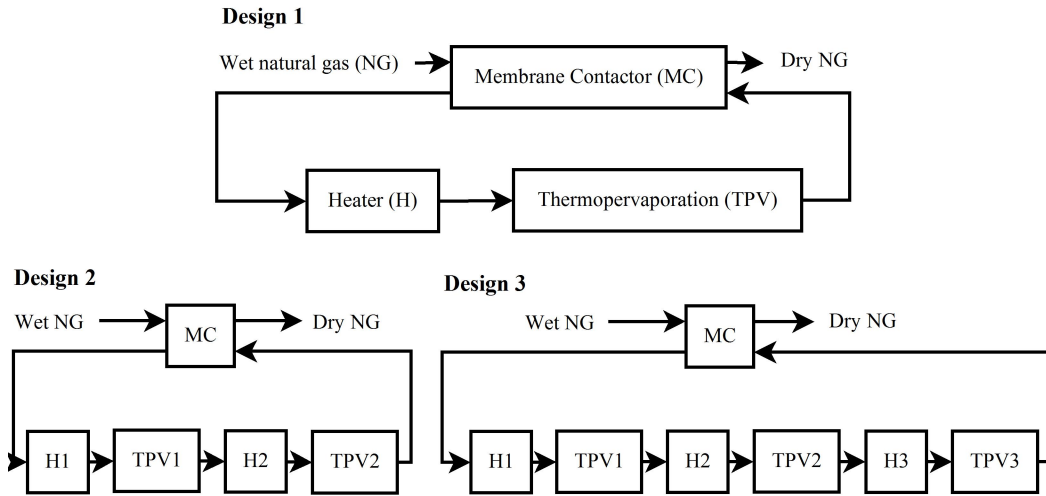


Figure 3: Simplified illustration of the three different design configurations of the dehydration process with one, two or three stages of regeneration. The illustration only shows the main differences between the designs, as the rest of the process is the same. MC indicates the membrane contactor, TPV is a thermopervaporation unit and H indicates an electrical heater.

163 The optimization is performed in MATLAB. Aspen HYSYS is accessed from MATLAB via activeX/COM  
 164 interface. Aspen HYSYS is used for the process simulation as different process configurations can easily be  
 165 simulated, in addition standard unit operations, flash calculations and thermodynamic properties can be  
 166 used. The optimization problem solved in MATLAB with the fmincon function can be written as:

$$\min_{\mathbf{x}} f(\mathbf{x}) \quad (1)$$

$$s.t. \quad \mathbf{c}(\mathbf{x}) \leq 0 \quad (2)$$

$$\mathbf{c}_{eq}(\mathbf{x}) = 0 \quad (3)$$

167 where  $f$  is the objective function to be minimized,  $\mathbf{c}$  is the inequality constraints,  $\mathbf{c}_{eq}$  is the equality  
 168 constraints and  $\mathbf{x}$  is the optimization variables. The main equality constraint is the dehydration pipeline

169 specification for the natural gas. The other constraints are mainly for simulation purposes to avoid infeasible  
 170 operation conditions. Every time Aspen HYSYS is called by the optimization routine it return values with  
 171 a given accuracy based on the solver tolerance for the membrane modules. To assure accurate results from  
 172 the optimization routine, the calculation tolerance of the membrane modules are given a much stricter  
 173 requirements than for the optimization. In addition, to avoid iterations in Aspen HYSYS the recycle block  
 174 is removed and equality constraints are added on the component molar flow of TEG and H<sub>2</sub>O to ensure that  
 175 the recycle loop is closed. The optimization variables ( $\mathbf{x}$ ), which are equal to the design variables are: molar  
 176 flow of TEG ( $f_{TEG}$ ) and H<sub>2</sub>O ( $f_{H_2O}$ ) in the regeneration loop at the membrane contactor inlet, number of  
 177 fibers in the membrane contactor ( $N_f$ ) and number of feed channels in the thermopervaporation unit(s) ( $N_c$ ).  
 178 The regeneration temperature of the TEG is also evaluated as an optimization variable. However, during  
 179 the first evaluation it is found that the temperature always reached the upper limit for the variable which  
 180 is decided based on material limitations. Therefore, the temperature is fixed to 100°C in the optimization  
 181 to reduce the computational time.

### 182 3.1. Objective function

183 The objective function to be minimized is a function based on investment and operating costs. The in-  
 184 vestment cost includes the main equipment in the regeneration loop, such as the membrane contactor, the  
 185 thermopervaporation unit(s), the heater(s) and the TEG recirculation pump. The operating cost includes  
 186 the electrical power required for the heater(s) and the pump in the TEG regeneration loop. The size of the  
 187 membrane unit(s) and the energy demand are parameters of interest. These are included in the objective  
 188 function as the investment cost of the membrane unit is proportional to the membrane area and the energy  
 189 consumption is included in the operating cost. The objective function is given in Eq. 4.

$$f = C_I \cdot ACCR + Q_{EL} \cdot C_{EL} \quad (4)$$

190 where  $C_I$  is the total capital cost,  $ACCR$  is the annual capital charge ratio,  $Q_{EL}$  is the annual electrical  
 191 power demands and  $C_{EL}$  is the electricity price.

192  
 193 A typical installation factor of six is used to estimate the total capital cost for fluid processes [65], **but to**  
 194 **adjust for the subsea conditions this factor is increased with 50%**. Based on this, the total capital cost can  
 195 be calculated with Eq. 5. However, this does not include the cost of the ships for the subsea installation,  
 196 which is not considered in this evaluation.

$$C_I = 9(C_{e,MC} + C_{e,TPV} + C_{e,P} + C_{e,H}) \quad (5)$$

197  $C_{e,MC}$  is the cost of the membrane contactor,  $C_{e,TPV}$  is the cost of the thermopervaporation unit(s),  $C_{e,P}$  is  
 198 the cost of the TEG recirculation pump and  $C_{e,H}$  is the cost of the electrical heater(s).

199  
 200 To include the capital cost in the objective function, it should be transformed to annual cost, which is  
 201 achieved with the use of the annual capital charge ratio (ACCR).

$$ACCR = \frac{[i(1+i)^n]}{[(1+i)^n - 1]} \quad (6)$$

202 where  $i$  is the interest rate and  $n$  is the number of years (lifetime of investment).

203  
 204 One uncertainty in this evaluation is the limitation in cost estimations for subsea processing equipment.  
 205 Therefore, onshore cost values are used with adjustment to include for subsea operation conditions. The  
 206 cost for the membrane contactor and thermopervaporation unit are assumed based on reported onshore  
 207 prices for membrane modules [66–68], with an increase by 50% to provide the more robust module shell for  
 208 subsea operation. The price of the thermopervaporation unit is assumed to be higher than the membrane  
 209 contactor based on more complexed module preparation with a lower packing density of the module. An  
 210 overview of the cost values and parameters in the objective function are given in Table 4.

Table 4: Cost values and parameters used in the objective function

Category	Parameter	Value
Capital Expenditure (CAPEX)	Membrane contactor cost ( $C_{e,MC}$ )	45 \$/m <sup>2</sup>
	Thermopervapoartion unit cost ( $C_{e,TPV}$ )	75 \$/m <sup>2</sup>
	Recirculation pump cost( $C_{e,P}$ )	Eq. 7
	Electrical heater cost ( $C_{e,H}$ )	Eq. 8
	Total fixed capital cost ( $C_I$ )	Eq.5
	Annual capital charge ratio (ACCR)	Eq.6
Annual Operating Expenditure (OPEX)	Electricity cost ( $C_{EL}$ )	0.0627 \$/kWh
Other assumptions	Equipment lifetime ( $n$ )	5 years
	Interest rate ( $i$ )	5%

211 The equipment cost of the TEG circulation pump ( $C_{e,P}$ ) and the electrical heater(s) ( $C_{e,H}$ ) are found based

212 on a linear approximation from cost estimation in Aspen HYSYS V9 given in Eq. 7 and Eq. 8 respectively.  
213 A factor of 50% is added to the equipment cost to adjust for the subsea conditions.

$$C_{e,P} = 1.5 (0.3872 \cdot S + 153,691) \quad (7)$$

$$C_{e,H} = 1.5 (2.0993 \cdot S + 8240.7) \quad (8)$$

214 Here,  $S$  is the size parameter, which for the recirculation pump is the liquid flow rate [L/s] and the for the  
215 electrical heater(s) is the energy demands [kW].

216

#### 217 4. Results and discussion

218 With the use of the `fmincon` function in MATLAB the optimum point with respect to the selected variables  
219 are found. Three different process designs are evaluated with different numbers of regeneration stages in the  
220 range from one to three, as illustrated in Fig. 3. The results from the optimization for the different process  
221 designs, including the values of the optimization variables are given in Table 5.

222

223 The temperature drop in the thermopervaporation unit affects the separation performance, due to the  
224 reduced driving force over the membrane. By introducing staging of the regeneration with heating between  
225 each thermopervaporation unit it is expected that the separation performance would be increased and provide  
226 a higher purity of the lean TEG. When the purity of the lean TEG is increased the required membrane  
227 area in the membrane contactor and the TEG flow rate is reduced. Reducing the TEG flow rate will also  
228 have an effect on the energy demand from the heaters and the pump. It is therefore expected that staging  
229 of the regeneration will provide a better design with respect to membrane sizes, TEG flow rate and energy  
230 demands. However, it is important to remember that increasing the number of stages introduces additional  
231 heaters, which increase the complexity. As expected, increasing the number of regeneration stages gives a  
232 decreased TEG flow rate as the purity of the lean TEG is increased. By increasing from one stage (Design 1)  
233 to two stages (Design 2) a larger benefit is provided compared to further increasing from two to three stages  
234 (Design 3). The TEG flow rate is reduced by 55.0% (353.6 kmol/h) for Design 2 compared to Design 1.  
235 Going from Design 2 to Design 3, a further reduction of 40.4% (116.7 kmol/h) is obtained. In conventional  
236 absorption dehydration processes a TEG circulation rate of 15-40 L<sub>TEG</sub>/kg<sub>H<sub>2</sub>O</sub>removed is commonly reported

237 [1, 69, 70]. This value is based on optimization of the conventional dehydration process, and it is important  
 238 to note that when new technologies are used for both the absorption and the regeneration step, this value  
 239 might not be an optimum for the new process. The results in Table 5 show that the TEG circulation rate for  
 240 all the evaluated designs are higher than the reported TEG circulation rate for the conventional absorption  
 241 process, but the value is reduced as the number of regeneration stages are increased.

Table 5: Values of the optimization variables and the result for the optimum point of the different process designs with respect to membrane sizes and energy demands. The volume calculation is based on only the active membrane area and a cooling wall thickness of 1 mm.

Parameter	Design 1	Design 2	Design 3	Unit
<b>Optimization variables</b>				
Molar flow TEG (fTEG)	590.6	267.1	160.0	[kmol/h]
Molar flow H <sub>2</sub> O (fH <sub>2</sub> O)	52.2	22.0	12.4	[kmol/h]
Number of MC fibers (Nf)	21.271	19.941	19.560	[x10 <sup>6</sup> ]
Number of TPV feed channels				
1 (Nc1)	8.206	3.374	1.915	[x10 <sup>3</sup> ]
2 (Nc2)		3.651	1.830	[x10 <sup>3</sup> ]
3 (Nc3)			2.105	[x10 <sup>3</sup> ]
<b>Results</b>				
Lean TEG flow rate	642.8	289.1	172.4	[kmol/h]
TEG circulation rate	197.8	89.4	53.5	[L <sub>TEG</sub> /kgH <sub>2</sub> O <sub>removed</sub> ]
Lean TEG purity	98.95	99.02	99.08	[wt%TEG]
MC area	40,095	37,588	36,869	[m <sup>2</sup> ]
MC volum	27	25	24.6	[m <sup>3</sup> ]
TPV area				
1	16,412	6784	3829	[m <sup>2</sup> ]
2		7123	3660	[m <sup>2</sup> ]
3			4209	[m <sup>2</sup> ]
TPV volum				
1	255	105	59	[m <sup>3</sup> ]
2		111	57	[m <sup>3</sup> ]
3			65	[m <sup>3</sup> ]
Total membrane volume	282	240	206	[m <sup>3</sup> ]
Heater duty				
1	4509	2048	1234	[kW]
2		797	471	[kW]
3			437	[kW]
Recirculation pump duty	243	110	66	[kW]
Total energy demand	4752	2955	2208	[kW]
Objective function value	9.45	7.85	7.06	[mill\$]

242

243 Increasing the number of regeneration stages also reduces the value of the objective function. Fig. 4  
 244 illustrates the contribution from the different parts of the objective function. From these results it can  
 245 be seen that the main contribution to the objective function is the cost of the membrane units and the  
 246 electricity. This explain why the value of the objective function is reduced with increased staging, even  
 247 though additional heaters are added. However, the contribution from the heater(s) to the objective function  
 248 is increased with the number of regeneration stages. Increasing the number of regeneration stages reduces  
 249 the contribution from the regeneration part (thermopervaporation unit(s), heater(s), recirculation pump  
 250 and electricity) of the objective function, while the membrane contactor percentage is increased.

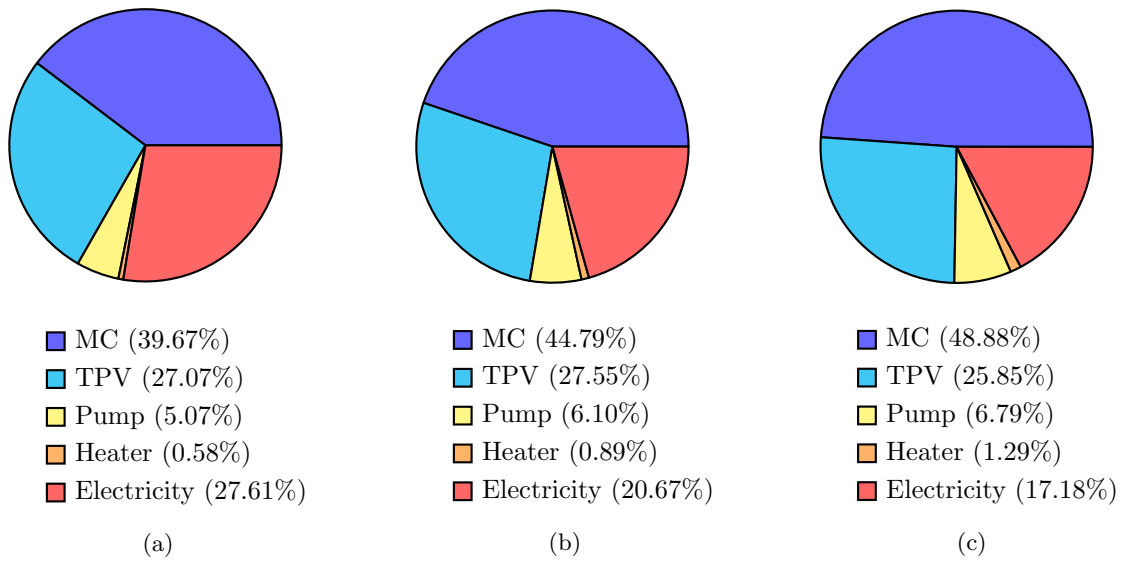


Figure 4: Contribution of the different parts on the cost function for the different process designs with respect to stages of regeneration; (a) Design 1 (one stage), (b) Design 2 (two stages) and (c) Design 3 (three stages). MC is an abbreviation for membrane contactor and TPV for thermopervaporation.

251 Important factors for subsea operation are the size of the system and the energy demand. As for the TEG  
 252 flow rate, increasing the number of stages reduces the total membrane volume and the energy demand.  
 253 Comparing the result of Design 1 and Design 2 shows that the total membrane volume is reduced by 14.6%  
 254 ( $41 \text{ m}^3$ ) and the total energy demand is reduced by 37.8% (1796 kW). Going from Design 2 to Design 3  
 255 gives a further decrease of the membrane volume by 14.3% ( $34 \text{ m}^2$ ) and 25.3% (747 kW) in the energy  
 256 requirements. The complexity of the system is increased with the additional heaters when the number of re-  
 257 generation stages is increased. In addition, the largest benefits are given when going from Design 1 to Design  
 258 2. Therefore, a further increase in number of regeneration stages might not be favorable. Compact design  
 259 is important due to installation and retrieval cost, in addition to limitations in weight for the installation  
 260 cranes. It is found that increasing the number of thermopervaporation stages is preferred from a separation

261 point of view. However, a next step for the practical evaluation of subsea installation is to evaluate how the  
 262 system should be designed in subsea installation modules. Big subsea modules would **require** a large ship  
 263 for the installation, while smaller modules would lead to more subsea connection **points** which **have** a larger  
 264 potential for leakages and failures. All these factors make it favorable to find the most compact design of  
 265 the process.

266  
 267 The results reveals that the low packing density of the thermopervaporation membrane module gives large  
 268 volumes for this units. Even though the membrane area in the membrane contactor is more than the double  
 269 of the thermopervaporation unit, the volume is much larger. The low packing density of the thermoperva-  
 270 poration unit ( $64.4 \text{ m}^2/\text{m}^3$ ) is based on the selected plate-and-frame module configuration, in addition to  
 271 the air gap and the cooling water channel which increases the size of the unit. From a practical point of  
 272 view, it could be favorable to reduce the size of the thermopervaporation unit and increase the membrane  
 273 contactor size to reduce the total membrane volume. An analysis is performed for Design 1, where the  
 274 number of fibers in the membrane contactor is changed simultaneously as the number of feed channels in the  
 275 thermopervaporation unit is **adjusted** to meet the dehydration criteria for the natural gas (Fig. 5a). In this  
 276 analysis the TEG flow rate is kept constant at the value found at the optimum point for Design 1 (Table  
 277 5). From the result given in Fig. 5b, it can be seen that the objective function has a minimum point as  
 278 reported above, however with respect to the total membrane volume, another minimum point can be found  
 279 (MC fibers  $32 \times 10^6$ ) with a higher value of the objective function.

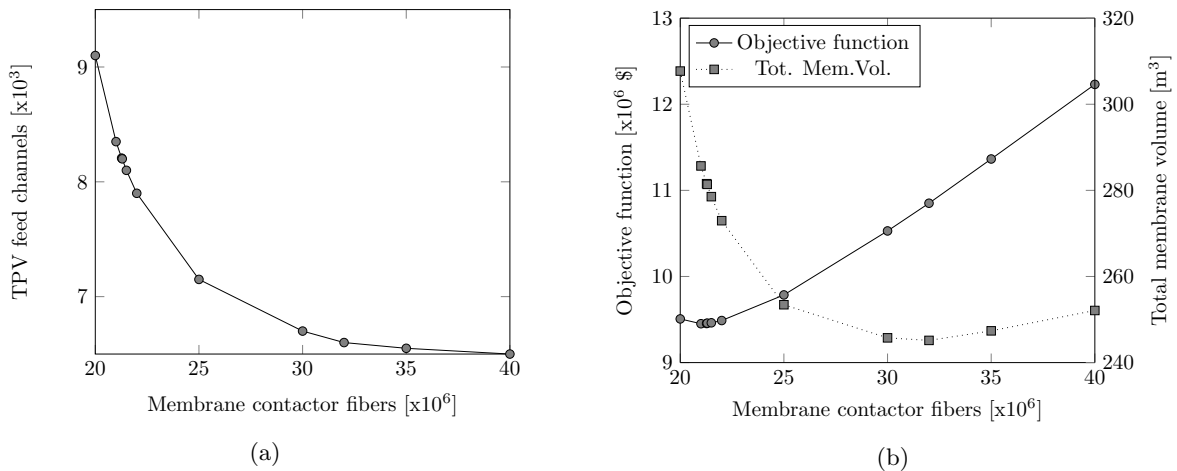


Figure 5: a) The number of feed channels in the thermopervaporation unit as a function of numbers of fibers in the membrane contactor, when the dehydration criteria for the natural gas is received. b) The value of the objective function and the total membrane volume (membrane contactor and thermopervaporation unit) as function of changing the number of fibers in the membrane contactor simultaneously as the number of feed channels in the thermopervaporation is adjusted.

280 The low packing density of the thermopervaporation module is related to the selection of membrane mod-  
281 ule, another module configuration, for instance tubular membrane modules, could provide a higher packing  
282 density and reduce the volume. The need for the air gap and the cooling water would still limit the packing  
283 density, but it is expected that the packing density would be higher. However, when changing the module  
284 configuration new models and evaluations of the module parameters are needed to evaluate the exact benefit  
285 on the packing density.

286  
287 The temperature drop and the low packing density of the thermopervaporation unit are two limiting **factors**  
288 for the proposed process. Adding spacers in the feed channels could increase the separation performance,  
289 as the introduction of mixing or turbulence might prevent or reduce the temperature and concentration  
290 polarization. This was proven by Krish et al. [71], for the butanol-water mixture and it is expected that  
291 the same effect might be seen for TEG-water mixtures. Another alternative that could be interesting to  
292 analyse is to introduce a heating channel or an electrical wire inside the feed channel to maintain the liquid  
293 temperature along the membrane module. However, if heating is placed close to the membrane material it is  
294 important to remember the temperature limitations for the membrane material. Avoiding the temperature  
295 drop could increase the separation performance and maybe a system as suggested in Design 1 without  
296 staging of the regeneration could be sufficient. This alternative moves the heating previously used between  
297 the regeneration stages to inside the membrane module, which means that the complexity of the system  
298 is moved to the membrane module and it is therefore a trade-off between system complexity or membrane  
299 module complexity.

#### 300 *4.1. Price sensitivity study*

301 As the cost values are based on assumptions and are uncertain values a sensitivity study for some of the  
302 parameters in the objective function was performed to evaluate how the optimum point is changed for Design  
303 2.

##### 304 *4.1.1. Price of thermopervaporation*

305 The price of the membrane units are related to the membrane area and therefore also to the size of the  
306 units. However, the thermopervaporation unit has a much lower packing density compared to the membrane  
307 contactor resulting in a much higher volume, even if the membrane area is much lower. In the objective  
308 function there is no penalty on the volume of the units, as the price is only related to the membrane area.  
309 As shown from the investigation for Design 1 (Fig. 5b) it was found that with respect to the total membrane



310 volume another minimum could be found. It is therefore of interest to evaluate how the optimum conditions  
 311 for the system are changing when the price of the thermopervaporation unit is increased, while keeping all  
 312 other cost values constant. Increasing the price difference between the membrane units will introduce a  
 313 penalty on the volume. In this sensitivity study four different prices were used for the thermopervaporation  
 314 unit; 75 (base case), 100 , 150 and 200  $\$/m^2$ .

315  
 316 The results given in Fig. 6 shows that increasing the price from 75 to 100 $\$/m^2$  do not change the optimum  
 317 point. But, as expected, with a further increase of the price the size of the thermopervaporation unit  
 318 is reduced. As the size of the thermopervaporation units are decreased, the total membrane volume is  
 319 reduced as the largest contribution is given by the thermopervaporation units (Fig. 6a). A decrease in the  
 320 regeneration size, results in a decreased purity of the lean TEG and hence an increase in the membrane  
 321 area in the membrane contactor, as illustrated in Fig. 6b. The lean TEG flow rate is increased when the  
 322 price is increased to 150  $\$/m^2$ . However, when the thermopervaporation price is further increased to 200  
 323  $\$/m^2$  a small reduction in the TEG flow rate can be seen, with a larger increase of the membrane area in  
 324 the membrane contactor.

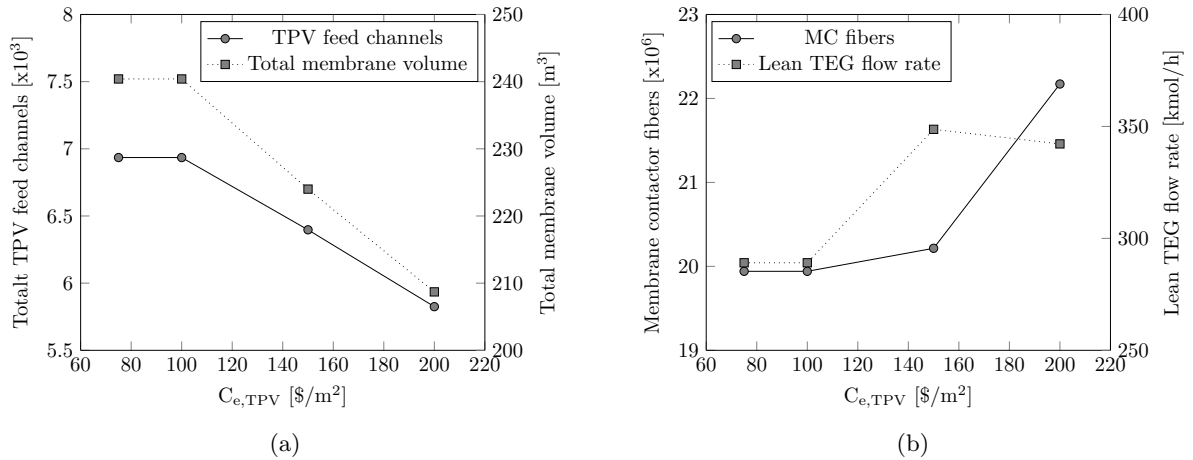


Figure 6: (a) The effect of the thermopervaporation cost on the total number of feed channels in the thermopervaporation units (TPV) and the total membrane volume (thermopervaporation units and membrane contactor). (b) The sizes of the membrane units with number of fibers in the membrane contactor (MC) and the lean TEG flow rate as function of the thermopervaporation cost.

#### 325 4.1.2. Electricity price

326 In the base case, the electricity price is set to 0.0627  $\$/kWh$ , for the sensitivity evaluation the price are  
 327 increased by 50% (0.0941 $\$/kWh$ ) and 100% (0.1254 $\$/kWh$ ). The results (Fig. 7) show that changing the  
 328 electricity price give some changes in the membrane sizes and TEG flow rate with respect to optimum design.

329 An increase in the electricity price results in a larger value of the objective function as the operating cost  
 330 is increased, and the values for the three cases are  $7.85 \times 10^6$  \$ (0.0627 \$/kWh),  $8.63 \times 10^6$  \$ (0.0941\$/kWh)  
 331 and  $9.36 \times 10^6$  \$ (0.1254\$/kWh). As the electricity price is increased a reduction of the TEG flow rate can  
 332 be seen of 7.9% and 14% compared to the base case when the electricity price is increased by 50 and  
 333 100% respectively. This is expected as a decrease in the flow rate is reducing the energy demands for the  
 334 heater(s) and the recirculation pump (Fig. 7a). A decrease in the TEG flow rate, requires an increase in  
 335 the membrane area for the membrane contactor (Fig. 7b) to be able to dehydrate the natural gas to the  
 336 pipeline specification.

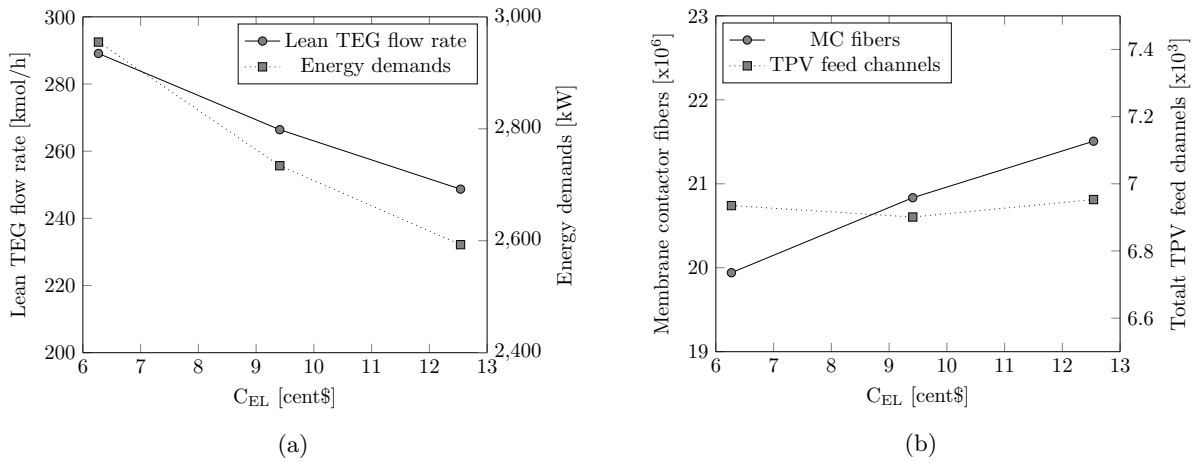


Figure 7: (a) The effect of the electricity cost on the lean TEG flow rate and the total energy demands. (b) The sizes of the membrane units with number of fibers in the membrane contactor (MC) and the total number of feed channels in the thermopervaporation units (TPV) as function of electricity cost.

## 337 5. Conclusion

338 A new process concept for subsea natural gas dehydration with membrane processes is evaluated, indicating  
 339 a promising potential for subsea operation. The proposed process is a regenerative design where a membrane  
 340 contactor is used for dehydration of natural gas with triethylene glycol (TEG) in combination with ther-  
 341 mopervaporation for regeneration of TEG. Three different process designs with staging of the regeneration  
 342 with heating between the stages are considered. Process optimization are performed and the result reveals  
 343 the following conclusions:

- 344 • Staging of the regeneration with heating between the stages are preferred as it reduces the size of the  
 345 membrane units, the energy demands and the TEG flow rate. Increasing the number of regeneration  
 346 stages from one to two gives a reduction of the TEG flow rate of 55% (353.6 kmol/h), in the total  
 347 membrane volume of 14.6% (41 m<sup>3</sup>) and in the energy requirements of 37.8% (1796 kW).

- 348 • The liquid temperature drop in the thermopervaporation unit is found to be a limiting factor for  
349 the system. The driving force over the membrane and the separation performance is reduced as the  
350 temperature drops. Therefore, staging of the regeneration would be preferred.
- 351 • Plate-and-frame module configuration for the thermopervaporation module provides a low packing  
352 density, which gives a large volume of the membrane unit.

## 353 Acknowledgement

354 This work was carried out as a part of SUBPRO (Subsea Production and Processing), a Research-based  
355 Innovation Centre within Subsea Production and Processing. The authors gratefully acknowledge the finan-  
356 cial support from SUBPRO, which is financed by the Research Council of Norway (237893), major industry  
357 partners and NTNU.

## 358 References

- 359 [1] Netusil M., Dittl P. Natural Gas Dehydration. In: Natural Gas - Extraction to End Use; chap. 1. InTech. ISBN  
360 978-953-51-0820-7; 2012, p. 223–63. URL: <http://linkinghub.elsevier.com/retrieve/pii/B9780128014998000079><http://www.intechopen.com/books/natural-gas-extraction-to-end-use/natural-gas-dehydration>. doi:10.5772/45802.
- 361
- 362 [2] Campbell J.M. Glycol Dehydration. In: Gas Conditioning and Processing; chap. 18. Oklahoma, USA; 1998, p. 333–94.
- 363 [3] GPSA Dehydration. In: Engineering Data Book; chap. 20. 2014, p. 20–1 – 20–54.
- 364 [4] Netusil M., Dittl P. Comparison of three methods for natural gas dehydration. Journal of Natural Gas  
365 Chemistry 2011;20(5):471–6. URL: [http://dx.doi.org/10.1016/S1003-9953\(10\)60218-6](http://dx.doi.org/10.1016/S1003-9953(10)60218-6). doi:10.1016/S1003-9953(10)  
366 60218-6.
- 367 [5] Ruud T., Idrac A., McKenzie L.J., Høy S.H. All Subsea: A Vision for the Future of Subsea Processing. In: Offshore  
368 Technology Conference. Offshore Technology Conference; 2015, URL: <http://www.onepetro.org/doi/10.4043/25735-MS>.  
369 doi:10.4043/25735-MS.
- 370 [6] Fredheim A.O., Johnsen C.G., Johannessen E., Kojen G.P. Gas-2-Pipe™, A Concept for Treating Gas to Rich  
371 Gas Quality in a Subsea or Unmanned Facility. In: Offshore Technology Conference. Offshore Technology Conference;  
372 2016, URL: <http://www.onepetro.org/doi/10.4043/27147-MS>. doi:10.4043/27147-MS.
- 373 [7] Jahnsen O., Storvik M., Kongsberg F. Subsea Processing & Boosting in a Global Perspective. In: Offshore Mediterranean  
374 Conference. Ravenna, Italy; 2011, p. 1–13.
- 375 [8] Albuquerque F., Ribeiro O., Morais M., Orłowski R., Vianna F., Kunchpil C., et al. Subsea Processing Systems:  
376 Future Vision. In: Offshore Technology Conference. Offshore Technology Conference; 2013, URL: <http://www.onepetro.org/doi/10.4043/24161-MS>. doi:10.4043/24161-MS.
- 377
- 378 [9] Orłowski R., Euphemio M.L.L., Euphemio M.L., Andrade C.A., Guedes F., Tosta da Silva L.C., et al. Marlim  
379 3 Phase Subsea Separation System - Challenges and Solutions for the Subsea Separation Station to Cope with Process  
380 Requirements. In: Offshore Technology Conference. Offshore Technology Conference. ISBN 978-1-61399-200-5; 2012,

- 381 p. 1–11. URL: <http://www.onepetro.org/mslib/app/Preview.do?paperNumber=OTC-23552-MS{&}societyCode=OTChttp://www.onepetro.org/doi/10.4043/23552-MS>. doi:10.4043/23552-MS.
- 382
- 383 [10] Dalane K., Dai Z., Mogseth G., Hillestad M., Deng L. Potential applications of membrane separation for subsea  
384 natural gas processing: A review. *Journal of Natural Gas Science and Engineering*2017;39:101–17. URL: <http://dx.doi.org/10.1016/j.jngse.2017.01.023>. doi:10.1016/j.jngse.2017.01.023.
- 385
- 386 [11] Boributh S., Rongwong W., Assabumrungrat S., Laosiripojana N., Jiraratananon R. Mathematical modeling and  
387 cascade design of hollow fiber membrane contactor for CO<sub>2</sub> absorption by monoethanolamine. *Journal of Membrane  
388 Science*2012;401-402:175–89. URL: <http://dx.doi.org/10.1016/j.memsci.2012.01.048>. doi:10.1016/j.memsci.2012.01.  
389 048.
- 390 [12] Rongwong W., Assabumrungrat S., Jiraratananon R. Rate based modeling for CO<sub>2</sub> absorption using monoethanolamine  
391 solution in a hollow fiber membrane contactor. *Journal of Membrane Science*2013;429:306–408. URL: <http://dx.doi.org/10.1016/j.memsci.2012.11.050>. doi:10.1016/j.memsci.2012.11.050.
- 392
- 393 [13] Rode S., Nguyen P.T., Roizard D., Bounaceur R., Castel C., Favre E. Evaluating the intensification potential of  
394 membrane contactors for gas absorption in a chemical solvent: A generic one-dimensional methodology and its appli-  
395 cation to CO<sub>2</sub> absorption in monoethanolamine. *Journal of Membrane Science*2012;389:1–16. URL: <http://dx.doi.org/10.1016/j.memsci.2011.09.042><http://linkinghub.elsevier.com/retrieve/pii/S0376738811007307>. doi:10.1016/  
396 j.memsci.2011.09.042.
- 397
- 398 [14] Albarracin Zaidiza D., Billaud J., Belaisaoui B., Rode S., Roizard D., Favre E. Modeling of CO<sub>2</sub> post-combustion  
399 capture using membrane contactors, comparison between one- and two-dimensional approaches. *Journal of Membrane  
400 Science*2014;455:64–74. URL: <http://dx.doi.org/10.1016/j.memsci.2013.12.012>. doi:10.1016/j.memsci.2013.12.012.
- 401 [15] Albarracin Zaidiza D., Belaisaoui B., Rode S., Neveux T., Makhloufi C., Castel C., et al. Adiabatic modelling of  
402 CO<sub>2</sub> capture by amine solvents using membrane contactors. *Journal of Membrane Science*2015;493:106–19. doi:10.1016/  
403 j.memsci.2015.06.015.
- 404 [16] Zhang H.Y., Wang R., Liang D.T., Tay J.H. Modeling and experimental study of CO<sub>2</sub> absorption in a hollow fiber  
405 membrane contactor. *Journal of Membrane Science*2006;279(1-2):301–10. URL: [http://www.sciencedirect.com/science/  
406 article/pii/S0376738805009051](http://www.sciencedirect.com/science/article/pii/S0376738805009051). doi:10.1016/j.memsci.2005.12.017.
- 407 [17] Hoff K.A. Modeling and Experimental Study of Carbon Dioxide Absorption in a Membrane Contactor. Ph.D. thesis;  
408 2003.
- 409 [18] Hoff K.A., Juliussen O., Falk-Pedersen O., Svendsen H.F. Modeling and Experimental Study of Carbon  
410 Dioxide Absorption in Aqueous Alkanolamine Solutions Using a Membrane Contactor. *Industrial & Engi-  
411 neering Chemistry Research*2004;43(16):4908–21. URL: [http://www.scopus.com/inward/record.url?eid=2-s2.  
412 0-3542993250{&}partnerID=40{&}md5=5135ac0a3b23c636a49dd913213c2d11](http://www.scopus.com/inward/record.url?eid=2-s2.0-3542993250{&}partnerID=40{&}md5=5135ac0a3b23c636a49dd913213c2d11)[http://pubs.acs.org/doi/abs/10.1021/  
413 ie034325a](http://pubs.acs.org/doi/abs/10.1021/ie034325a). doi:10.1021/ie034325a.
- 414 [19] Boucif N., Corriou J.P., Roizard D., Favre E. Carbon dioxide absorption by monoethanolamine in hollow fiber membrane  
415 contactors: A parametric investigation. *AIChE Journal*2012;58(9):2843–55. doi:10.1002/aic.12791.
- 416 [20] Eslami S., Mousavi S.M., Danesh S., Banazadeh H. Modeling and simulation of CO<sub>2</sub> removal from power plant flue  
417 gas by PG solution in a hollow fiber membrane contactor. *Advances in Engineering Software*2011;42(8):612–20. URL:  
418 <http://dx.doi.org/10.1016/j.advengsoft.2011.05.002>. doi:10.1016/j.advengsoft.2011.05.002.
- 419 [21] Faiz R., Al-Marzouqi M. CO<sub>2</sub> removal from natural gas at high pressure using membrane contactors: Model val-

- 420 idation and membrane parametric studies. *Journal of Membrane Science*2010;365(1-2):232–41. URL: <http://dx.doi.org/10.1016/j.memsci.2010.09.004><http://linkinghub.elsevier.com/retrieve/pii/S0376738810007015>. doi:10.1016/
- 421 [j.memsci.2010.09.004](http://dx.doi.org/10.1016/j.memsci.2010.09.004).
- 422
- 423 [22] Faiz R., Al-Marzouqi M. Mathematical modeling for the simultaneous absorption of CO<sub>2</sub> and H<sub>2</sub>S using MEA in hollow
- 424 fiber membrane contactors. *Journal of Membrane Science*2009;342(1-2):269–78. doi:10.1016/j.memsci.2009.06.050.
- 425 [23] Yan Y., Zhang Z., Zhang L., Chen Y., Tang Q. Dynamic Modeling of Biogas Upgrading in Hollow Fiber Membrane
- 426 Contactors. *Energy & Fuels*2014;28(9):5745–55. URL: <http://pubs.acs.org/doi/abs/10.1021/ef501435q>. doi:10.1021/
- 427 [ef501435q](http://pubs.acs.org/doi/abs/10.1021/ef501435q).
- 428 [24] Rezakazemi M., Niazi Z., Mirfendereski M., Shirazian S., Mohammadi T., Pak A. CFD simulation of natural gas
- 429 sweetening in a gas-liquid hollow-fiber membrane contactor. *Chemical Engineering Journal*2011;168(3):1217–26. URL:
- 430 <http://dx.doi.org/10.1016/j.cej.2011.02.019>. doi:10.1016/j.cej.2011.02.019.
- 431 [25] Razavi S.M.R., Razavi S.M.J., Miri T., Shirazian S. CFD simulation of CO<sub>2</sub> capture from gas mixtures in
- 432 nanoporous membranes by solution of 2-amino-2-methyl-1-propanol and piperazine. *International Journal of Greenhouse*
- 433 *Gas Control*2013;15:142–9. URL: <http://dx.doi.org/10.1016/j.ijggc.2013.02.011>. doi:10.1016/j.ijggc.2013.02.011.
- 434 [26] Zhang Z., Yan Y., Zhang L., Chen Y., Ran J., Pu G., et al. Theoretical Study on CO<sub>2</sub> Absorption from Biogas by
- 435 Membrane Contactors : Effect of Operating Parameters. *Industrial & Engineering Chemistry Research*2014;
- 436 [27] Chabanon E., Roizard D., Favre E. Modeling strategies of membrane contactors for post-combustion carbon capture:
- 437 A critical comparative study. *Chemical Engineering Science*2013;87:393–407. URL: <http://dx.doi.org/10.1016/j.ces.2012.09.011>.
- 438 [2012.09.011](http://dx.doi.org/10.1016/j.ces.2012.09.011). doi:10.1016/j.ces.2012.09.011.
- 439 [28] Albarracin Zaidiza D., Wilson S.G., Belaisaoui B., Rode S., Castel C., Roizard D., et al. Rigorous modelling of
- 440 adiabatic multicomponent CO<sub>2</sub> post-combustion capture using hollow fibre membrane contactors. *Chemical Engineering*
- 441 *Science*2016;145:45–58. URL: <http://dx.doi.org/10.1016/j.ces.2016.01.053>. doi:10.1016/j.ces.2016.01.053.
- 442 [29] Boributh S., Assabumrungrat S., Laosiripojana N., Jiratananon R. A modeling study on the effects of membrane
- 443 characteristics and operating parameters on physical absorption of CO<sub>2</sub> by hollow fiber membrane contactor. *Journal*
- 444 *of Membrane Science*2011;380(1-2):21–33. URL: <http://linkinghub.elsevier.com/retrieve/pii/S0376738811004686>.
- 445 [doi:10.1016/j.memsci.2011.06.029](http://linkinghub.elsevier.com/retrieve/pii/S0376738811004686).
- 446 [30] Farjami M., Moghadassi A., Vatanpour V. Modeling and simulation of CO<sub>2</sub> removal in a polyvinylidene fluoride
- 447 hollow fiber membrane contactor with computational fluid dynamics. *Chemical Engineering and Processing: Process*
- 448 *Intensification*2015;98:41–51. doi:10.1016/j.cep.2015.10.006.
- 449 [31] Dai Z., Usman M., Hillestad M., Deng L. Modelling of a tubular membrane contactor for pre-combustion CO<sub>2</sub>
- 450 capture using ionic liquids: Influence of the membrane configuration, absorbent properties and operation parameters.
- 451 *Green Energy and Environment*2016;1(3):266–75. URL: <http://dx.doi.org/10.1016/j.gee.2016.11.006>. doi:10.1016/
- 452 [j.gee.2016.11.006](http://dx.doi.org/10.1016/j.gee.2016.11.006).
- 453 [32] Usman M., Dai Z., Hillestad M., Deng L. Mathematical modeling and validation of CO<sub>2</sub> mass transfer in a membrane
- 454 contactor using ionic liquids for pre-combustion CO<sub>2</sub> capture. *Chemical Engineering Research and Design*2017;123:377–87.
- 455 URL: <http://linkinghub.elsevier.com/retrieve/pii/S0263876217303155>. doi:10.1016/j.cherd.2017.05.026.
- 456 [33] Usman M., Hillestad M., Deng L. Assessment of a membrane contactor process for pre-combustion CO<sub>2</sub> capture by
- 457 modelling and integrated process simulation. *International Journal of Greenhouse Gas Control*2018;71(December 2017):95–
- 458 [103](https://doi.org/10.1016/j.ijggc.2018.02.012). URL: <https://doi.org/10.1016/j.ijggc.2018.02.012>. doi:10.1016/j.ijggc.2018.02.012.

- 459 [34] Falk-Pedersen O., Grønvold M.S., Nøkleby P., Bjerve F., Svendsen H.F. CO<sub>2</sub> Capture with Membrane Contactors. *International Journal of Green Energy*2005;2(2):157–65. URL: <http://www.tandfonline.com/doi/abs/10.1081/GE-200058965>.  
460  
461 doi:10.1081/GE-200058965.
- 462 [35] Meyer H.S., Palla R., King S.I. Field Tests Support Reliability of Membrane Gas/Liquid Contactor Gas Dehydration  
463 System. *Gas Technology Institute*2002;8:37–40.
- 464 [36] King S.I., Falk-Pedersen O., Stuksrud D.B., Grønvold M.S., Svendsen H.F., Palla R., et al. Membrane Gas/Liquid  
465 Contactors for Natural Gas Dehydration. In: *The 52nd Annual Laurance Reid Gas Conditioning Conference*. 2002,.
- 466 [37] Wijmans I.J.G., Park M., Wijmans J.G., Ng A., Mairal A.P. Natural Gas Dehydration Process and Apparatus. 2004.
- 467 [38] Wu X.M., Guo H., Soyekwo F., Zhang Q.G., Lin C.X., Liu Q.L., et al. Pervaporation Purification of Ethylene  
468 Glycol Using the Highly Permeable PIM-1 Membrane. *Journal of Chemical & Engineering Data*2016;61(1):579–86. URL:  
469 <http://pubs.acs.org/doi/abs/10.1021/acs.jced.5b00731>. doi:10.1021/acs.jced.5b00731.
- 470 [39] Hu C., Li B., Guo R., Wu H., Jiang Z. Pervaporation performance of chitosan–poly(acrylic acid) polyelectrolyte complex  
471 membranes for dehydration of ethylene glycol aqueous solution. *Separation and Purification Technology*2007;55(3):327–34.  
472 URL: <http://linkinghub.elsevier.com/retrieve/pii/S1383586607000408>. doi:10.1016/j.seppur.2007.01.005.
- 473 [40] Guo R., Hu C., Li B., Jiang Z. Pervaporation separation of ethylene glycol/water mixtures through surface crosslinked  
474 PVA membranes: Coupling effect and separation performance analysis. *Journal of Membrane Science*2007;289(1-2):191–8.  
475 URL: <http://linkinghub.elsevier.com/retrieve/pii/S0376738806008052>. doi:10.1016/j.memsci.2006.11.055.
- 476 [41] Guo R., Hu C., Pan F., Wu H., Jiang Z. PVA–GPTMS/TEOS hybrid pervaporation membrane for dehydration of  
477 ethylene glycol aqueous solution. *Journal of Membrane Science*2006;281(1-2):454–62. URL: <http://linkinghub.elsevier.com/retrieve/pii/S0376738806002511>. doi:10.1016/j.memsci.2006.04.015.
- 478
- 479 [42] Burshe M., Sawant S., Joshi J., Pangarkar V. Dehydration of ethylene glycol by pervaporation using hydrophilic  
480 IPNs of PVA, PAA and PAAM membranes. *Separation and Purification Technology*1998;13(1):47–56. URL: <http://linkinghub.elsevier.com/retrieve/pii/S1383586697000610>. doi:10.1016/S1383-5866(97)00061-0.
- 481
- 482 [43] Wang Y., Chung T.S., Neo B.W., Gruender M. Processing and engineering of pervaporation dehydration of ethylene  
483 glycol via dual-layer polybenzimidazole (PBI)/polyetherimide (PEI) membranes. *Journal of Membrane Science*2011;378(1-  
484 2):339–50. URL: <http://dx.doi.org/10.1016/j.memsci.2011.05.020><http://linkinghub.elsevier.com/retrieve/pii/S0376738811003577>. doi:10.1016/j.memsci.2011.05.020.
- 485
- 486 [44] Ong Y.T., Tan S.H. Synthesis of the novel symmetric buckypaper supported ionic liquid membrane for the dehydration  
487 of ethylene glycol by pervaporation. *Separation and Purification Technology*2015;143:135–45. URL: <http://dx.doi.org/10.1016/j.seppur.2015.01.021><http://linkinghub.elsevier.com/retrieve/pii/S1383586615000507>. doi:10.1016/  
488 [j.seppur.2015.01.021](http://dx.doi.org/10.1016/j.seppur.2015.01.021).
- 489
- 490 [45] Rao P.S., Sridhar S., Wey M.Y., Krishnaiah A. Pervaporative Separation of Ethylene Glycol/Water Mixtures by Using  
491 Cross-linked Chitosan Membranes. *Industrial & Engineering Chemistry Research*2007;46(7):2155–63. URL: <http://pubs.acs.org/doi/pdf/10.1021/ie061268n><http://pubs.acs.org/doi/abs/10.1021/ie061268n>. doi:10.1021/ie061268n.
- 492
- 493 [46] Xu J., Gao C., Feng X. Thin-film-composite membranes comprising of self-assembled polyelectrolytes for separation of  
494 water from ethylene glycol by pervaporation. *Journal of Membrane Science*2010;352(1-2):197–204. URL: <http://dx.doi.org/10.1016/j.memsci.2010.02.017><http://linkinghub.elsevier.com/retrieve/pii/S0376738810001067>. doi:10.1016/  
495 [j.memsci.2010.02.017](http://dx.doi.org/10.1016/j.memsci.2010.02.017).
- 496
- 497 [47] Hua G., Falcone G., Teodoriu C., Morrison G. Comparison of Multiphase pumping technologies for subsea and

- 498 downhole applications. *Oil and Gas Facilities*2012;(February):36–46. URL: <https://www.onepetro.org/journal-paper/SPE-146784-PA>. doi:10.2118/146784-MS.
- 499
- 500 [48] Won Yim D., Kong S.H. Pervaporative dehydration of diethylene glycol through a hollow fiber membrane. *Journal of Applied Polymer Science*2013;129(1):499–506. URL: <http://doi.wiley.com/10.1002/app.38603>. doi:10.1002/app.38603.
- 501
- 502 [49] Hu C., Guo R., Li B., Ma X., Wu H., Jiang Development of novel mordenite-filled chitosan–poly(acrylic acid) polyelectrolyte complex membranes for pervaporation dehydration of ethylene glycol aqueous solution. *Journal of Membrane Science*2007;293(1-2):142–50. URL: <http://linkinghub.elsevier.com/retrieve/pii/S0376738807001007>. doi:10.1016/j.memsci.2007.02.009.
- 503
- 504
- 505
- 506 [50] Yu C., Zhong C., Liu Y., Gu X., Yang G., Xing W., et al. Pervaporation dehydration of ethylene glycol by NaA zeolite membranes. *Chemical Engineering Research and Design*2012;90(9):1372–80. URL: <http://dx.doi.org/10.1016/j.cherd.2011.12.003><http://linkinghub.elsevier.com/retrieve/pii/S0263876211004734>. doi:10.1016/j.cherd.2011.12.003.
- 507
- 508
- 509 [51] Dogan H., Durmaz Hilmioglu N. Chitosan coated zeolite filled regenerated cellulose membrane for dehydration of ethylene glycol/water mixtures by pervaporation. *Desalination*2010;258(1-3):120–7. URL: <http://dx.doi.org/10.1016/j.desal.2010.03.027><http://linkinghub.elsevier.com/retrieve/pii/S0011916410001621>. doi:10.1016/j.desal.2010.03.027.
- 510
- 511
- 512 [52] Jafari M., Bayat A., Mohammadi T., Kazemimoghadam M. Dehydration of ethylene glycol by pervaporation using gamma alumina/NaA zeolite composite membrane. *Chemical Engineering Research and Design*2013;91(12):2412–9. URL: <http://dx.doi.org/10.1016/j.cherd.2013.04.016><http://linkinghub.elsevier.com/retrieve/pii/S0263876213001433>. doi:10.1016/j.cherd.2013.04.016.
- 513
- 514
- 515
- 516 [53] Akberov R.R., Fazlyev A.R., Klinov A.V., Malygin A.V., Farakhov M.I., Maryakhina V.A., et al. Dehydration of diethylene glycol by pervaporation using HybSi ceramic membranes. *Theoretical Foundations of Chemical Engineering*2014;48(5):650–5. URL: <http://link.springer.com/10.1134/S0040579514030014>. doi:10.1134/S0040579514030014.
- 517
- 518
- 519
- 520 [54] Hyder M., Chen P. Pervaporation dehydration of ethylene glycol with chitosan–poly(vinyl alcohol) blend membranes: Effect of CS–PVA blending ratios. *Journal of Membrane Science*2009;340(1-2):171–80. URL: <http://linkinghub.elsevier.com/retrieve/pii/S0376738809003780>. doi:10.1016/j.memsci.2009.05.021.
- 521
- 522
- 523 [55] Hyder M., Huang R., Chen P. Composite poly(vinyl alcohol)–poly(sulfone) membranes crosslinked by trimesoyl chloride: Characterization and dehydration of ethylene glycol–water mixtures. *Journal of Membrane Science*2009;326(2):363–71. URL: <http://linkinghub.elsevier.com/retrieve/pii/S0376738808008971>. doi:10.1016/j.memsci.2008.10.017.
- 524
- 525
- 526 [56] Sun D., Yang P., Sun H.L., Li B.B. Preparation and characterization of cross-linked poly (vinyl alcohol)/hyperbranched polyester membrane for the pervaporation dehydration of ethylene glycol solution. *European Polymer Journal*2015;62:155–66. URL: <http://dx.doi.org/10.1016/j.eurpolymj.2014.11.027><http://linkinghub.elsevier.com/retrieve/pii/S0014305714004121>. doi:10.1016/j.eurpolymj.2014.11.027.
- 527
- 528
- 529
- 530 [57] van Veen H., van Delft Y., Engelen C., Pex P. Dewatering of organics by pervaporation with silica membranes. *Separation and Purification Technology*2001;22-23(1-2):361–6. URL: <http://linkinghub.elsevier.com/retrieve/pii/S1383586600001192>. doi:10.1016/S1383-5866(00)00119-2.
- 531
- 532
- 533 [58] Josefsen N.T. Subsea regeneration of triethylene glycol (TEG) for natural gas dehydration. Ph.D. thesis; Norwegian University of Science and Technology; 2017.
- 534
- 535 [59] Dalane K., Josefsen N.T., Ansaloni L., Hillestad M., Deng L. Thermopervaporation for regeneration of triethylene glycol ( TEG ): Experimental and model development. *Submitter to Journal of Membrane Science*2018;.
- 536

- 537 [60] Dalane K., Svendsen H.F., Hillestad M., Deng L. Membrane contactor for subsea natural gas dehydration: Model devel-  
538 opment and sensitivity study. *Journal of Membrane Science*2018;556(March):263–76. URL: [https://doi.org/10.1016/j.](https://doi.org/10.1016/j.memsci.2018.03.033)  
539 [memsci.2018.03.033](https://doi.org/10.1016/j.memsci.2018.03.033)<http://linkinghub.elsevier.com/retrieve/pii/S0376738818300115>. doi:10.1016/j.memsci.2018.  
540 03.033.
- 541 [61] AmsterChem Matlab CAPE-OPEN Unit Operation. 2017. URL: <https://www.amsterchem.com/matlabunitop.html>.
- 542 [62] Gassco Terms and conditions for transportation of gas in GASSLED, Valid from 1 Jan-  
543 uary 2018. 2018. URL: [http://www.gassco.no/contentassets/40e7d932034346caaa7ac647bcd9ee6f/](http://www.gassco.no/contentassets/40e7d932034346caaa7ac647bcd9ee6f/terms-and-conditions-for-transportation-of-gas-in-gassled---01.01.2018.pdf)  
544 [terms-and-conditions-for-transportation-of-gas-in-gassled---01.01.2018.pdf](http://www.gassco.no/contentassets/40e7d932034346caaa7ac647bcd9ee6f/terms-and-conditions-for-transportation-of-gas-in-gassled---01.01.2018.pdf).
- 545 [63] van Baten J., Pons M. CAPE-OPEN: Interoperability in Industrial Flowsheet Simulation Software. *Chemie Ingenieur*  
546 *Technik*2014;86(7):1052–64. URL: <http://doi.wiley.com/10.1002/cite.201400009>. doi:10.1002/cite.201400009.
- 547 [64] CO-LaN The CAPE-OPEN Standard. 2017. URL: <http://www.colan.org/>.
- 548 [65] Towler G., Sinnott R. *Chemical engineering design*. Elsevier; 2008. ISBN 9780750684231. URL: [http://linkinghub.](http://linkinghub.elsevier.com/retrieve/pii/B9780080966595000225)  
549 [elsevier.com/retrieve/pii/B9780080966595000225](http://linkinghub.elsevier.com/retrieve/pii/B9780080966595000225). arXiv:arXiv:1011.1669v3.
- 550 [66] Haider S., Lindbräthen A., Lie J.A., Andersen I.C.T., Hägg M.B. CO<sub>2</sub>separation with carbon membranes in high  
551 pressure and elevated temperature applications. *Separation and Purification Technology*2018;190(August 2017):177–89.  
552 URL: <http://dx.doi.org/10.1016/j.seppur.2017.08.038>. doi:10.1016/j.seppur.2017.08.038.
- 553 [67] Merkel T.C., Lin H., Wei X., Baker R. Power plant post-combustion carbon dioxide capture: An opportunity for  
554 membranes. *Journal of Membrane Science*2010;359(1-2):126–39. URL: [http://dx.doi.org/10.1016/j.memsci.2009.10.](http://dx.doi.org/10.1016/j.memsci.2009.10.041)  
555 [041](http://dx.doi.org/10.1016/j.memsci.2009.10.041). doi:10.1016/j.memsci.2009.10.041.
- 556 [68] He X., Fu C., Hägg M.B. Membrane system design and process feasibility analysis for CO<sub>2</sub>capture from flue gas with a  
557 fixed-site-carrier membrane. *Chemical Engineering Journal*2015;268:1–9. URL: [http://dx.doi.org/10.1016/j.cej.2014.](http://dx.doi.org/10.1016/j.cej.2014.12.105)  
558 [12.105](http://dx.doi.org/10.1016/j.cej.2014.12.105). doi:10.1016/j.cej.2014.12.105.
- 559 [69] Bahadori A. Natural Gas Dehydration. In: *Natural Gas Processing*; chap. 9. Elsevier. ISBN 9780080999715; 2014, p. 441–  
560 81. URL: <http://linkinghub.elsevier.com/retrieve/pii/B978008099971500009X>. doi:10.1016/B978-0-08-099971-5.  
561 [00009-X](http://linkinghub.elsevier.com/retrieve/pii/B978008099971500009X).
- 562 [70] Mokhatab S., Poe W.A., Speight J.G. Natural gas dehydration. In: Mokhatab S., Poe W.A., Speight J.G., editors.  
563 *Handbook of Natural Gas Transmission and Processing*; chap. 9. Elsevier; 2006, p. 323–64. URL: [http://linkinghub.](http://linkinghub.elsevier.com/retrieve/pii/B9780750677769500142)  
564 [elsevier.com/retrieve/pii/B9780750677769500142](http://linkinghub.elsevier.com/retrieve/pii/B9780750677769500142). doi:10.1016/B978-075067776-9/50014-2.
- 565 [71] Kirsh V., Borisov I., Volkov V. Hydrodynamics of a thermopervaporation flow membrane module with cylindrical  
566 spacers. *Petroleum Chemistry*2013;53(8):578–84. doi:10.1134/S0965544113080070.